

*Citation for published version:*

Cal, L., Suarez-Bregua, P., Braasch, I., Irion, U., Kelsh, R., Cerdá-Reverter, JM & Rotllant, J 2019, 'Loss-of-function mutations in the melanocortin 1 receptor cause disruption of dorso-ventral countershading in teleost fish', *Pigment Cell and Melanoma Research*, vol. 32, no. 6, pp. 817-828. <https://doi.org/10.1111/pcmr.12806>

*DOI:*

[10.1111/pcmr.12806](https://doi.org/10.1111/pcmr.12806)

*Publication date:*

2019

*Document Version*

Peer reviewed version

[Link to publication](https://doi.org/10.1111/pcmr.12806)

This is the peer reviewed version of the following article: Cal, L., Suarez-Bregua, P., Braasch, I., Irion, U., Kelsh, R., Cerdá-Reverter, J. M., & Rotllant, J. (2019). Loss-of-function mutations in the melanocortin 1 receptor cause disruption of dorso-ventral countershading in teleost fish. *Pigment Cell and Melanoma Research*, which has been published in final form at <https://doi.org/10.1111/pcmr.12806> . This article may be used for non-commercial purposes in accordance with Wiley Terms and Conditions for Self-Archiving.

**University of Bath**

## **Alternative formats**

If you require this document in an alternative format, please contact:  
[openaccess@bath.ac.uk](mailto:openaccess@bath.ac.uk)

### **General rights**

Copyright and moral rights for the publications made accessible in the public portal are retained by the authors and/or other copyright owners and it is a condition of accessing publications that users recognise and abide by the legal requirements associated with these rights.

### **Take down policy**

If you believe that this document breaches copyright please contact us providing details, and we will remove access to the work immediately and investigate your claim.

**Loss-of-function mutations in the melanocortin-1-receptor (Mc1r) cause disruption of dorso-ventral countershading in teleost fish**

Laura Cal<sup>1</sup>, Paula Suarez-Bregua<sup>1</sup>, Ingo Braasch<sup>2</sup>, Uwe Irion<sup>3</sup>, Robert Kelsh<sup>4</sup>, Jose Miguel Cerdá-Reverter<sup>5\*&</sup>, Josep Rotllant<sup>1\*&</sup>.

Short title: Fish pigmentation and melanocortin system

<sup>1</sup> FishBioTech Lab. Department of Biotechnology & Aquaculture. Institute of Marine Research, (IIM-CSIC), 36208 Vigo, Spain.

<sup>2</sup>Department of Integrative Biology and Program in Ecology, Evolutionary Biology and Behavior, Michigan State University, East Lansing, MI 48824, USA.

<sup>3</sup>Max-Planck-Institut of Developmental Biology, Tübingen, Germany

<sup>4</sup>Department of Biology and Biochemistry and Centre for Regenerative Medicine, University of Bath, Claverton Down, Bath, BA2 7AY, United Kingdom.

<sup>5</sup>Department of Fish Physiology and Biotechnology, Institute of Aquaculture from Torre la Sal (IATS-CSIC), Castellon, Spain. 12595, Spain.

\*Corresponding authors and reprint requests:

Josep Rotllant, Instituto de Investigaciones Marinas, CSIC. Eduardo Cabello, 36208, Vigo (Pontevedra), Spain

Tel. (+34) 986-231930 Fax (+34) 986 292 762

E-mail: [rotllant@iim.csic.es](mailto:rotllant@iim.csic.es)

25 Jose Miguel Cerdá-Reverter, Instituto de Acuicultura de Torre de la Sal, CSIC. Torre  
26 la Sal s/n, 12595, Ribera de Cabanes, Castellón, Spain  
27 Tel. (+34) 964319500 Fax (+34) 964319509  
28 E-mail: jm.cerda.reverter@csic.es  
29  
30 &Co-senior authors

31    **ABSTRACT**

32    The Melanocortin 1 receptor (MC1R) is the central melanocortin receptor involved in  
33    vertebrate pigmentation. Mutations in this gene cause variations in coat coloration in  
34    amniotes. Additionally, in mammals MC1R is the main receptor for agouti signaling  
35    protein (ASIP), making it the critical receptor for the establishment of dorsal-ventral  
36    countershading. In fish, *Mc1r* is also involved in pigmentation but it has been almost  
37    exclusively studied in relation to melanosome dispersion activity and as a putative  
38    genetic factor involved in dark/light adaptation. However, its role as the crucial  
39    component for the *Asip1*-dependent control of dorsal-ventral pigmentation remains  
40    unexplored. Using CRISPR/Cas9 we created *mc1r* homozygous knockout zebrafish  
41    and found that loss-of-function of *mc1r* causes a reduction of countershading and a  
42    general paling of the animals. We find ectopic development of melanophores and  
43    xanthophores, accompanied by a decrease in iridophore numbers in the ventral region  
44    of *mc1r* mutants. We also reveal subtle differences in the role of *mc1r* in repressing  
45    pigment cell development between the skin and scale niches in ventral regions

46  
47    **Keywords:** *Mc1r*, *Asip1*, pigmentation, melanophores, xanthophores, iridophores,  
48    chromatophore, zebrafish, countershading, CRISPR

49  
50    **SIGNIFICANCE**

51    Countershading is a widespread pigmentary adaptation throughout vertebrates and  
52    graded agouti-signaling peptide (ASIP) is the main regulatory effector. In mammals,  
53    *Asip* expression signals through melanocortin receptor type-1 (MC1R) to inhibit  
54    melanogenesis and melanocyte differentiation *in vitro*. Strikingly, in fish *Asip*-  
55    dependent dorso-ventral patterning depends upon multiple types of chromatophore,

56 but the skin expresses multiple MCRs and the role for Mc1r remains untested. We  
57 show here that Mc1r is required to block melanophore and xanthophore, and to  
58 promote iridophore, development in ventral skin. In contrast, loss of Mc1r function  
59 only partially reduced melanophores and xanthophores dorsally, suggesting  
60 involvement of additional signaling systems.

61

## 62 **INTRODUCTION**

63 Pigment patterns have always intrigued scientists for both their evolutionary and  
64 developmental aspects, and fish constitute excellent models because of their great  
65 color pattern diversity. Zebrafish (*Danio rerio*) has become an important model to  
66 study color pattern formation and cell fate decisions in vertebrates. Its striped  
67 pigmentation is achieved by the patterned distribution of three types of pigment cells  
68 (chromatophores), melanophores, xanthophores and iridophores. Both melanophores  
69 and xanthophores absorb light due to the synthesis of melanin and pteridine pigments,  
70 respectively; whereas iridophores reflect light because of guanine crystals (Hirata et  
71 al., 2003, Hirata et al., 2005) . This striped pattern is superimposed on an ancient dorso-  
72 ventral countershading pattern, with dark dorsum and light ventrum (Cal et al., 2017;  
73 Ceinos et al., 2015). Dorso-ventral pigment polarity is a highly conserved evolutionary  
74 trait (Linnen et al., 2013). It is regulated by the local presence/absence of agouti-  
75 signaling protein (ASIP, simply called Agouti in mouse) (Vrieling et al., 1994). In  
76 mammals ASIP binds to the melanocortin receptor 1 (MC1R), encoded by the  
77 extension (e) locus, and which is the receptor for melanin-stimulating hormone (MSH)  
78 (Robbins et al., 1993). Binding of agouti to MC1R lowers the ratio of eumelanin  
79 (dark/brown pigment) to pheomelanin (red/yellow pigment) produced in the  
80 melanocytes (mammalian melanophores) (Michaud et al., 1993; Miller et al., 1993),

81 inhibits melanoblast differentiation and proliferation (Aberdam et al., 1998;  
82 Sviderskaya et al., 2001) and promotes dedifferentiation of melanocytes *in vitro* (Le  
83 Pape et al., 2009). Agouti expression in different regions of the body is controlled by  
84 distinct regulatory regions of the agouti gene. It results in either ventral specific or hair  
85 cycle specific isoforms controlled by distinct regulatory enhancer regions of the *agouti*  
86 gene. These result in either ventral specific or hair cycle specific isoforms. The ventral  
87 isoform is constitutively expressed during development thus driving melanocytes to  
88 synthesize pheomelanin and resulting in pale coloration. Dorsal-specific isoform  
89 expression is temporally regulated during the hair cycle, thus producing the distinctive  
90 yellow subapical band of the agouti fur coloration (Vrieling et al., 1994). Dorsoventral  
91 pigmentation gradients in fish also depend on a dorso-ventral expression gradient of  
92 *Asip1* (the fish ortholog of mammalian ASIP) (Cerdá-Reverter et al., 2005; Ceinos et  
93 al., 2015; Guillot et al., 2012;), but the cellular and biochemical mechanisms seem to  
94 be different from that of mammalian species. Fish melanophores synthesize only  
95 eumelanin (Kottler et al., 2015), therefore changes in dorsoventral pigmentation can  
96 be achieved either by inhibition of melanogenesis or by differential chromatophore  
97 distribution. In zebrafish, *asip1* overexpression inhibits melanogenesis in the dorsal  
98 region (Ceinos et al., 2015; Guillot et al., 2012) by antagonizing melanocortin  
99 signaling (Cerdá-Reverter., 2005), but it also promotes the proliferation of dorsal  
100 iridophores (Ceinos et al., 2015). Accordingly, *asip1* knockout has no effect on dorsal  
101 pigmentation but the lack of *Asip1* in the belly promotes a dorsalization of the ventral  
102 pigmentation by increasing melanophore differentiation and xanthophore numbers in  
103 parallel with the disappearance of most ventral iridophores (Cal et al., 2019). Taken  
104 together, the gradient of *asip1* expression is responsible for the dorso-ventral

105 pigmentation gradient in fish by using a different mechanism from tetrapods, i.e. by  
 106 inhibiting ventral melanogenesis and modulating chromatoblast fate.  
 107 This analysis leaves an important question concerning the signaling mechanism that  
 108 Asip1 uses in zebrafish to regulate pigmentation. To date, five different melanocortin  
 109 receptors (Mc1r-Mc5r) have been characterized in vertebrates (Cortés et al., 2014).  
 110 Mc2r is unique because it is exclusively activated by the adrenocorticotrophic hormone  
 111 (ACTH) and it requires the interaction with the melanocortin receptor accessory  
 112 protein 1 (Mrap1) (Cerdá-Reverter et al., 2013). All other receptors bind the diverse  
 113 MSH-ligands with different affinities (Schiöth et al., 2005), and ACTH can also  
 114 activate Mc4r in combination with Mrap2 (Agulleiro et al., 2013). Asip1 has been  
 115 shown to antagonize the effects of Msh on Mc1r and Mc4r in goldfish (Cerdá-Reverter  
 116 et al., 2005). In addition, Asip1 can inhibit (Nle4, D-Phe7)- $\alpha$ -MSH-stimulated  
 117 melanosome dispersion (Cerdá-Reverter et al., 2005). Zebrafish has six melanocortin  
 118 receptors, since Mc5r is duplicated, as Mc5ra and Mc5rb (Cortés et al., 2014). They are  
 119 antagonized by Asip1 but the protein seems to work also as an inverse agonist at Mc1r  
 120 (Guillot et al., 2012), with low Mc1R activity occurring in the absence of MSH or the  
 121 presence of Asip1. Although the involvement of Mc1r signaling in the agouti  
 122 phenotype of zebrafish has been suggested, we cannot rule out the participation of  
 123 other Mcr receptors since their expression in fish skin has been reported, e.g. Mc4r in  
 124 cyprinids (Cerdá-Reverter et al., 2003; Wei et al., 2013), Mc5r in flatfishes, goldfish,  
 125 and bass (Cerdá-Reverter et al., 2003; Kobayashi et al., 2012; Sánchez et al., 2009)  
 126 and Mc2r in bass (Agulleiro et al., 2013). Here, we investigate the role of Mc1r in  
 127 zebrafish pigmentation *in vivo* by generating knockout mutants using the  
 128 CRISPR/Cas9 genome-editing tool (Bassett et al., 2013). We demonstrate a disruption  
 129 of the dorso-ventral pigmentation polarity in *mc1r* knock-out fish, consistent with it

130 being the key receptor mediating *Asip1* function in zebrafish dorsoventral  
131 countershading.

132

## 133 **MATERIALS AND METHODS**

### 134 **Fish**

135 Zebrafish were cultured as previously described (Westerfield., 2007) and staged by  
136 standard criteria (Kimmel et al., 1995). Fish of the following genotypes were used: Tü  
137 strain (Tübingen, Nüsslein-Volhard Lab), Tg(Xla.Eef1a1:Cau.*Asip1*)iim05 (Ceinos et  
138 al., 2015), Tg(TDL358:GFP)(Levesque et al., 2013) , Tg(kita:GalTA4:UAS:mCherry)  
139 (Anelli et al., 2009). Ethical approval (Ref. Number: AGL2011-23581) for all studies  
140 was obtained from the Institutional Animal Care and Use Committee of the IIM-CSIC  
141 Institute in accordance with the National Advisory Committee for Laboratory Animal  
142 Research Guidelines licensed by the Spanish Authority (RD53/2013) and conformed  
143 to European animal directive (2010/63/UE) for the protection of experimental animals.

144

### 145 **Generation and analysis of *mc1r* knockout mutants**

146 The *mc1r* loss-of-function mutation was generated using the CRISPR-Cas9 gene  
147 editing system. The CRISPR protocol, originally adapted from Bassett et al. (Bassett  
148 et al., 2013), was kindly provided by Sam Peterson (U Oregon). The possible target  
149 sequence was identified with the ChopChop web tool (Montague et al., 2014). Two  
150 long oligonucleotides (Scaffold oligo: 5'-  
151 GATCCGCACCGACTCGGTGCCACTTTTTCAAGTTGATAACGGACTAGCCT  
152 TATTTTAACTTGCTATTTCTAGCTCTAAAAC-3', and two different gene-  
153 specific oligo GS1: 5'-  
154 AATTAATACGACTCACTATAGCTAGTGAGCGTCAGTAATGGTTTTAGAGC



155 TAGAAATAGC-3' and GS2: 5'-  
 156 AATTAATACGACTCACTATAGGGCCAAGATGAACATGTGCAGGGTTTTAG  
 157 AGCTAGAAATAGC-3' ) were used to perform a template-free PCR to obtain a 125  
 158 bp DNA fragment that includes the two previously identified target site sequences  
 159 (TS1: 5'- GCTAGTGAGCGTCAGTAATGTGG-3' and TS2: 5'-  
 160 GGGCCAAGATGAACATGTGCAGG-3'). The PCR reaction was performed in 20  
 161 µL containing 10 µL of 2x Phusion High-Fidelity PCR Master Mix Buffer (New  
 162 England Biolabs, UK), 1 µL of gene specific oligo (10 µM), 1 µL of gRNA scaffold  
 163 oligo (10 µM) and H<sub>2</sub>O nuclease free to 20 µL. PCR conditions were 98°C for 30 sec,  
 164 40 cycles of 98°C for 10 sec, 60°C for 10 sec, 72°C for 15 sec, and a final step of 72°C  
 165 for 10 min. The PCR product was purified using DNA Clean&Concentration-5 Kit  
 166 (Zymo Research, USA) according to the manufacturer's instructions. Purified PCR  
 167 product was used as template for in vitro transcription with MEGAscript T7 High yield  
 168 transcription Kit (Ambion, USA) according to the manufacturer's instructions. The  
 169 gRNA was purified with RNA Clean&Concentrator 5 (Zymo Research, USA). The  
 170 gRNA was injected in a concentration of 25 ng/µL together with Cas9 mRNA (from  
 171 the pT3TS-nCas9n plasmid, Addgene, USA) at 50 ng/µL and Phenol red solution  
 172 (0,1%). Around 2 nL of this mix was microinjected into zebrafish eggs. Different  
 173 mutations were found and three different potential non-functional mutations were  
 174 raised as separate mutant allele lines (see results section). Primer sequence for  
 175 genotyping PCR were: TS1-F: CTTCAGCATGAAACACATGGA; TS1-R:  
 176 ATGGTGCACAGAAACGACAA; TS2-F: CTTCAGCATGAAACACATGGA;  
 177 TS2-R: AAGGGTTTGTGGGACAGGTG. For microscope imaging, zebrafish of  
 178 5dpf, 15 dpf, 30 dpf and 210 dpf were anesthetized with tricaine methasulfonate (MS-  
 179 222-, Sigma-Aldrich), skin sections and scales were isolated from the ventral and

dorsal areas and immersed in PBS on a glass slide and photographed. Transgenic/mutant lines were obtained by setting up crosses between the *mc1r* mutant lines and the reporter transgenic line Tg(TDL358:GFP), which labels iridophores (Levesque et al., 2013), or Tg(kita:GalTA4:UAS:mCherry), which labels melanophores (Anelli et al., 2009). The offspring of these crosses were incrossed to obtain homozygous *mc1r* mutants. Confocal imaging was carried out on a Leica TCS SP5 confocal microscope.

### **Melanophore and xanthophore counts**

The melanophore pattern of *mc1r* knockout mutant fish (*mc1r*<sup>K.O.</sup>) was compared with control fish by quantification of melanized melanophores in both groups (Fig. 3, 4). Selected regions for melanophore counting were different in each stage of development. In early stage (5dpf), we counted melanophores in a 1 mm<sup>2</sup> area in a dorsal view on the head and the dorsal area, on the horizontal myoseptum and in a ventral view of the head. In early metamorphic stage (15dpf), we counted melanophores in a 1 mm<sup>2</sup> area in a dorsal view on the head, on the dorsal area, on the horizontal myoseptum and in a ventral view of the head and the belly. In late metamorphic stage (30dpf), we counted melanophores in a 1 mm<sup>2</sup> area in a dorsal view on the head, dorsal area, horizontal myoseptum and in a ventral view on the head and belly. In adult fish (60 and 210 dpf) melanophores within 1 mm<sup>2</sup> area were counted in several distinct positions: in a dorsal view on the head (head area) and on the dorsal area (from the edge of the head to edge of the dorsal fin); in a lateral view, on the dorsalmost dark stripe (2D), 1D, first ventral dark stripe under the myoseptum (1V) and 2V anterior areas (pectoral to pelvic fin); and finally, in a ventral view of the head and the belly (pectoral to pelvic fin) (see Fig. 4A; Fig 7Q-T). The dorsal-ventral

205 xanthophore pattern of *mc1r* knockout fish mutant was compared with control fish by  
 206 quantification of pigmented xanthophores in post-metamorphic fish (60 and 210 dpf).  
 207 For xanthophore counting, selected regions on the dorsal area (from the edge of the  
 208 head to edge of the dorsal fin), and in a ventral view of the belly (pectoral to pelvic  
 209 fin) were selected (see Fig. 4A). To analyze the number of melanophores and  
 210 xanthophores, seven fish per group were anesthetized with tricaine methasulfonate  
 211 (MS-222-, Sigma-Aldrich) and immersed in 10 mg/ml epinephrine (Sigma) solution  
 212 for 30 min to contract melanosomes. Fish were photographed on a Leica M165FC  
 213 stereomicroscope equipped with a Leica DFC310FX camera. Melanophores were  
 214 counted using ADOBE PHOTOSHOP CS2 software (Adobe Systems Software Adobe  
 215 Systems Ibérica SL, Barcelona, Spain) and the ImageJ software (National Institutes of  
 216 Health, NIH, Maryland, USA). Data values were statistically evaluated by Student's  
 217 t-test and data expressed as mean standard error of the mean (SEM).

218

#### 219 **Functional *Asip1/Mc1r* interaction**

220 Transgenic/knockout line (*mc1r<sup>K.O.</sup>/Asip1-Tg*) were obtained by setting up crosses  
 221 between the CRISPR1-*mc1r.iim02* mutant line and the transgenic reporter line  
 222 Tg(Xla.Eef1a1:Cau.*Asip1*)iim05 (Ceinos et al., 2015), which ectopically  
 223 overexpresses *asip1* and produces a dorsal-ventral disruption of pigment pattern  
 224 phenotype with dorsal skin as pale colored as ventral skin. The offspring was then  
 225 incrossed to obtain the F2 generation and the *mc1r* locus was sequenced to confirm  
 226 the homozygous knockout mutation (*mc1r<sup>K.O.</sup>*) that carries the dominant *asip1*  
 227 transgene, localized by PCR using specific primers for the Tol2 vector (forward: 5'-  
 228 GCCCCTCTGCTAACCATGTTC-3', reverse: 5'-  
 229 TCATCAATGTATCTTATCATGTCTGG-3'). Adult double transgenic/mutant

zebrafish (100dpf) were anesthetized with MS-222 and photographed. Microscope imaging was carried out in a Leica M165FC stereomicroscope equipped with a Leica DFC310FX camera.

## RESULTS

### Generation and selection of induced *mc1r* loss-of-function mutations

Loss-of-function mutations in the zebrafish *mc1r* gene were generated using the CRISPR/Cas9 system. We selected two different target sites in the single coding exon (target T1: 286 bp after ATG and target T2: 636 bp after ATG) (Fig. 1A, B) and found six different mutated alleles (Fig. 1B). Alleles M1 and M6 conserved the original open reading frame; therefore, they could potentially generate a functional protein lacking only one or two amino acids but keeping most of the complete amino acid sequence. Alleles M2, M3, M4 and M5 show different open reading frames downstream of the target site. The *mc1r* gene encodes a predicted protein of 323 amino acids. We selected three mutations with predicted non-functional protein and established stable homozygous mutant lines of each one to characterize the phenotype: M2 (CRISPR1-*mc1r.iim02*), M3 (CRISPR1-*mc1r.iim03*), and M4 (CRISPR1-*mc1r.iim04*) (Fig. 1B). The *mc1r<sup>iim02</sup>* allele lacks 7 bp (Del 264-271) and carries 11 bp insertion at position 264 downstream of the predicted ATG. The *mc1r<sup>iim03</sup>* allele has lost 2 bp (Del 642-644), and *mc1r<sup>iim04</sup>* lacks 2 bp (Del 642-644) and carries 16 bp insertion at position 642 downstream of the predicted ATG (Fig. 1B). In those three alleles, the mutations result in premature stop codons. The *mc1r<sup>iim02</sup>* encodes a 123 amino acids mutant protein with 95 shared amino acids with WT Mc1r, the *mc1r<sup>iim03</sup>* encodes a mutant protein with 231 amino acids with 214 shared amino acids with WT Mc1r, and *mc1r<sup>iim04</sup>* encodes a mutant protein with 243 amino acids with 214 shared amino acids

255 with WT Mc1r (Fig. 1C). None of the predicted mutated proteins have the last three  
256  $\alpha$ -helical transmembrane (TM) domains and an intracellular C-terminus with a  
257 palmitoylation site which are required for ligand-receptor binding and the appropriate  
258 tertiary structure of the receptor, therefore none of these mutant proteins would be  
259 predicted to retain partial function. All *mc1r* knockout mutant lines examined resulted  
260 in a similar dorso-ventral pigment phenotype as described below.

261

### 262 ***mc1r* functions in dorso-ventral pigment patterning**

263 All three homozygous *mc1r*-CRISPR knockout lines exhibited an indistinguishable  
264 reduction of dorso-ventral countershading (Fig. 2), therefore we focused on the study  
265 of one homozygous line, CRISPR1-*mc1r*.iim02 (referred to as *mc1r<sup>K.O.</sup>*). *mc1r<sup>K.O.</sup>* fish  
266 displayed enhanced pigmentation over the entire ventral region (Fig. 2 B, D, F, H), as  
267 well as a significant reduction over the dorsal and lateral regions (Fig. 2 D, J) compared  
268 to WT siblings. In particular, in *mc1r<sup>K.O.</sup>* fish, the number of melanophores and  
269 xanthophores is increased in all ventral regions (Fig 2. G, H) together with a  
270 concomitant reduction of these two pigment cell types in all dorsal regions (Fig.2 I, J).  
271 This phenotype results in an apparent paling of the animal with a corresponding  
272 reduction of countershading. Mutations of the *mc1r* gene had no major effect on the  
273 characteristic striped pattern (Fig.2 A-D). However, we observe a significant decrease  
274 of melanophore numbers in the dorsal 2D dark stripe, and the incipient 3V-stripe is  
275 more pronounced in *mc1r<sup>K.O.</sup>* mutants compared to wild type (Fig. 2C,D). In addition,  
276 the abdominal ventral region exhibits a decrease in the number of iridophores that  
277 results in an apparent breakup of the ventral iridophore layer into smaller fragments,  
278 thus conferring a darker color to the ventral region of *mc1r<sup>K.O.</sup>* fish (Fig. 2H).

279

## 280    **The development of the zebrafish *mc1r<sup>K.O.</sup>* phenotype**

281    To establish the time point when the phenotype of the *mc1r<sup>K.O.</sup>* mutants first becomes  
282    apparent during development, melanophores were counted at larval (5dpf, SL 3 mm),  
283    metamorphic (15 dpf, SL 6.3 mm and 30 dpf, SL 7 mm) and two adult stages (60 dpf,  
284    SL 13 mm and 210 dpf, SL 25 mm) (Fig. 3 and 4). It has been shown that pigment  
285    pattern changes during development can be quantified by an increase in melanophore  
286    numbers and variations in their distribution (Kelsh., 2004; Parichy et al., 2009) . We  
287    determined the melanophore distribution in *mc1r<sup>K.O.</sup>* and WT siblings along the dorso-  
288    ventral axis, by counting at defined positions in the dorsal and ventral head, the lateral  
289    stripes and the belly (see Materials and Methods and Figs. 3 and 4 for details). We  
290    found a significant general reduction of melanophore density in *mc1r<sup>K.O.</sup>* at all  
291    developmental stages evaluated. At pre-metamorphic (15dpf) and metamorphic stages,  
292    the melanophore density were significantly lower in all areas examined. During pre-  
293    metamorphic stages (15dpf), melanophore density was lower in the dorsal, lateral and  
294    belly regions of *mc1r<sup>K.O.</sup>* mutants compared to WT fish (Fig. 3A). During late  
295    metamorphosis (30dpf), melanophore density was also lower in the dorsal, lateral  
296    region and belly of *mc1r<sup>K.O.</sup>* mutants compared to WT fish (Fig. 3B). At adult stages  
297    (60 and 210 dpf), *mc1r<sup>K.O.</sup>* mutants exhibited an obvious dorso-ventral pigmentation  
298    defect characterized by an increase of melanophore and xanthophore density in the  
299    ventral areas (Fig. 4B) together with a significant decrease of melanophore and  
300    xanthophore density in the dorsal and lateral body sections, resulting in a general  
301    homogenization of melanophores densities across the dorsoventral axis (Fig. 4C). At  
302    60 dpf, the density of melanophores in *mc1r<sup>K.O.</sup>* mutants compared to WT fish was  
303    lower in the dorsal region, the dark stripe 2D, the dark stripe 1D and in the dark stripe  
304    1V. However, in the ventral region of the head, the density of melanophores was higher

305 in *mc1r<sup>K.O.</sup>* mutants compared to WT fish. No differences were found in the dark stripe  
 306 2V and the belly (Fig. 4C). Additionally, the density of xanthophores was also  
 307 affected. *mc1r<sup>K.O.</sup>* mutants show a significant increase in the number of ventral  
 308 xanthophores ( $P < 0.01$ ) compared to WT fish (Fig. 4D). A similar phenotype was  
 309 found at 210 dpf; melanophore densities in 210 dpf *mc1r<sup>K.O.</sup>* mutants were  
 310 considerably lower in the dorsal region of the head, in the dorsal region, in the dark  
 311 stripe 2D and in the dark stripe 1D compared to WT. In contrast, the density of  
 312 melanophores in the ventral region, in the dark stripe 3V and in the belly of *mc1r<sup>K.O.</sup>*  
 313 fish was significantly higher than in their WT siblings (Fig. 4E). The density of  
 314 xanthophores in the dorsal region of *mc1r<sup>K.O.</sup>* mutants was lower than in WT fish.  
 315 However, the density of xanthophores in the ventral regions of *mc1r<sup>K.O.</sup>* fish was  
 316 considerably higher than in WT fish (Fig. 4F).  
 317 We also compared the distribution of transgenic markers for melanophores and  
 318 iridophores in *mc1r<sup>K.O.</sup>* mutants and their WT siblings to assess densities of possible  
 319 unpigmented pigment cells or their precursors. Firstly, we imaged fish carrying the  
 320 Tg(Kita:GalTA4,UAS:mCherry) transgene, which labels melanophores with  
 321 membrane-bound mCherry (Anelli et al., 2009). WT fish showed no pigmented  
 322 melanophores in the ventral skin (Fig. 5A, B), but there were also no unpigmented  
 323 mCherry-expressing cells suggesting a complete absence of melanophores and  
 324 melanoblasts (Fig. 5B). In contrast, *mc1r<sup>K.O.</sup>* mutants showed an increase in mCherry  
 325 labelled melanophores in the ventral skin region (Fig. 5C, D). This is in agreement  
 326 with the detected increase in the number of melanophores in ventral regions (Fig. 4).  
 327 By analyzing fish carrying Tg(TDL358:GFP), a transgene labeling iridophores and  
 328 glia with cytosolic GFP (Levesque et al., 2013), we confirmed the presence of a dense  
 329 and uniform sheet of iridophores in the ventral abdominal skin of WT fish (Figs. 5E,

330 F) and showed that this layer is broken up into smaller fragments in *mc1r<sup>K.O.</sup>* mutants  
331 (Fig. 5G, H). Although it is difficult to quantify the contribution of changed cell  
332 numbers to this phenotype, *mc1r<sup>K.O.</sup>* mutants display a significant reduction of the  
333 extent of iridophores, together with a significantly increased number of melanophores  
334 and xanthophores (Fig. 5G) within the ventral abdominal skin.  
335 Finally, we characterized the contribution of pigment cells in the scales to the disrupted  
336 countershading and pale phenotype in *mc1r<sup>K.O.</sup>* mutants. Scales isolated from the  
337 dorsum of *mc1r<sup>K.O.</sup>* mutants displayed a substantial reduction of melanophores (Fig.  
338 6B, black arrowheads) compared to WT fish (Fig. 6A). In contrast to ventral scales of  
339 WT siblings which lack all pigmented cell-types (Fig. 6C), ventral scales from *mc1r<sup>K.O.</sup>*  
340 mutants display some ectopic melanophores (Fig. 6D, black arrowheads) and  
341 numerous xanthophores (Fig. 6D, yellow arrowheads).

342

### 343 **Zebrafish *Asip1* is likely acting as an inverse agonist of Mc1r**

344 To determine if *Asip1* signaling is mediated by Mc1r, we analyzed the combination of  
345 *mc1r<sup>K.O.</sup>* with the *asip1*-Tg zebrafish line that overexpresses *asip1* in the entire body.  
346 We predicted that, if *Asip1* signaling functions solely through Mc1r that the *mc1r<sup>K.O.</sup>*/  
347 *asip1*-Tg fish would show a pattern identical to the *mc1r<sup>K.O.</sup>* line, whereas if another  
348 receptor contributed to *Asip1* signaling, the pattern would be more similar to the *asip1*-  
349 Tg line. Both *mc1r<sup>K.O.</sup>* and *asip1*-Tg zebrafish lines differ significantly in their overall  
350 pigmentation phenotype compared to WT fish (Fig. 7). WT fish (Fig. 7A) show a  
351 specific striped pattern (Fig. 7 B), a light ventrum (Fig. 7C) and a darker dorsum (Fig.  
352 7D). In *mc1r<sup>K.O.</sup>* mutants (Fig. 7E) the striped pattern is barely affected (Fig. 7F), but  
353 they show a darker belly (Fig. 7G) and a paler dorsum with fewer melanophores than  
354 WT fish (Fig. 7 H,R). The *asip1*-Tg zebrafish phenotype presents a slightly affected



355 striped pattern (Fig 7J), a light belly similar to WT fish (Fig. 7K), but a drastic  
356 reduction of dorsal melanophores (Fig. 7L,S) due to the ectopic overexpression of  
357 *asip1* (Ceinos et al., 2015). In the combination of *mc1r<sup>K.O.</sup>* with *asip1*-Tg, the *asip1*-  
358 Tg phenotype is suppressed and the *mc1r<sup>K.O.</sup>* phenotype prevails (Fig. 7M). The  
359 *mc1r<sup>K.O.</sup>* + *asip1*-Tg zebrafish line presented the same barely affected stripe pattern  
360 like *mc1r<sup>K.O.</sup>* alone (Fig. 7 N), the pigmented belly (Fig. 7O) and the dark dorsum with  
361 similar numbers of melanophores as the *mc1r<sup>K.O.</sup>* fish (Fig. 7P,T). Fish overexpressing  
362 *asip1* are paler than fish lacking Mc1r. This suggests that Asip1 has additional effects  
363 to those promoted by Mc1r, either by competitive antagonism or inverse agonism, as  
364 the overexpression phenotype is stronger than absence of the receptor. Fish that  
365 overexpress Asip1 but also lack Mc1r have a ventrally dorsalized pigmentation  
366 phenotype, similar to fish only lacking Mc1r, indicating that Asip1 is probably acting  
367 as an inverse agonist of Mc1r to elicit the opposite response from that produced by  $\alpha$ -  
368 Msh. Additionally, scales isolated from the dorsum of the *mc1r<sup>K.O.</sup>/ asip1*-Tg fish  
369 displayed a similar substantial reduction of melanophores than *mc1r<sup>K.O.</sup>* mutants (Fig.  
370 S1A,C) compared to WT fish (Fig. 6A) and an increase of melanophores compared to  
371 *asip1*-Tg fish (Fig.S1B) . Ventral scales from *mc1r<sup>K.O.</sup>/ asip1*-Tg also showed some  
372 melanophores and numerous xanthophores (Fig. S1F).

373

## 374 **DISCUSSION**

375 Zebrafish, a major teleost fish model for pigmentation studies, utilizes two distinct  
376 mechanisms to generate the adult pigmentation, the striped patterning and the dorso-  
377 ventral countershading mechanism (Ceinos et al., 2015). Both mechanisms function  
378 largely independently, with the resultant patterns superimposed to give the full pattern  
379 (Ceinos et al., 2015). The dorso-ventral expression gradient of *asip1* is responsible for

the countershading, through inhibition of melanogenesis in the ventral region where *asip1* is highly expressed. However, *Asip1* is also involved in the regulation of chromatophore numbers since its overexpression modifies the melanophore/iridophore ratio by promoting iridophore differentiation in absence of melanophores (Ceinos et al., 2015). Our previous studies have demonstrated that *Asip1* works as a competitive antagonist of both *Mc1r* and *Mc4r* (Cerdá-Reverter et al., 2005; Guillot et al., 2016) but likely also as an inverse agonist of the constitutively activated *Mc1r* (Guillot et al., 2016; Sánchez et al., 2010). *Asip1* overexpression in zebrafish results in a ventralization of the dorsal skin pigmentation due to a substantial reduction in the number of melanophores and the concomitant production of extra iridophores, without effects on the ventral pigmentation (Ceinos et al., 2015). In blind Mexican cave tetra (*Astyanax mexicanus*) *Mc1r* plays a key role in the establishment of the adult pigment pattern; inactivating mutations are responsible for the reduction in the number of melanophores, a phenotype that can be recapitulated in zebrafish by *mc1r* morpholino knockdown (Gross et al., 2009). We now demonstrate that inactivating mutations of *mc1r* in zebrafish lead to a reduction in the number of dorsal melanophores, and that also extends to the dorsalmost stripe. In addition they lead to a significant reduction in the number of dorsal xanthophores during all post-metamorphic stages studied. If *Asip1* works as an inverse agonist of the constitutively activated *Mc1r*, inactivating mutations of the cognate receptor would be predicted to recapitulate the *asip1-Tg* dorsal effect. However, the number of dorsal melanophores in *asip1-Tg* fish was less reduced in an *mc1r<sup>K.O.</sup>* background when compared to a WT background. Also, *asip1-Tg* zebrafish exhibit an extra dorsal band of iridophores (Ceinos et al., 2015), which is absent in *mc1r<sup>K.O.</sup>* mutants. Therefore, overexpression of *asip1* in *mc1r<sup>K.O.</sup>* background yields a similar phenotype to that of *mc1r* knockout mutant unmasking what is

405 essentially an epistatic relationship between *asip1* and *mc1r*. Our data demonstrate  
406 that *Asip1* displays a more pronounced effect when *Mc1r* is present and suggests that  
407 the effect is more than simply blocking of the constitutive activity of *Mc1r* (Ollmann  
408 et al., 1998). Similar results have been reported in mouse showing that individuals  
409 ubiquitously expressing high levels of *asip* exhibit paler yellow fur than that seem  
410 when *mc1r* is absent (Ollmann et al., 1998; Jackson et al., 2007).

411 The dorsal root ganglia (DRG) host multipotent stem cells that can generate all three  
412 pigment-cell types found in the post-metamorphic skin of zebrafish (Singh et al.,  
413 2016). These stem cells remain multipotent until well into metamorphosis when  
414 individual pigment cell fates become specified (Singh et al., 2016). Under our original  
415 model, the constitutive or MSH-induced activation of *Mc1r* promotes melanocyte fate  
416 decisions and differentiation in the dorsal skin, but in the more ventral regions, the  
417 inverse agonism or competitive antagonism of *Asip1* would block *Mc1r* activity,  
418 instead promoting the differentiation of iridophores. Accordingly, we would expect  
419 the phenotype of the *asip1-Tg* line (where *Mc1r* inactivation is driven by dorsal  
420 overexpression of *asip1*) to be similar to the phenotype of the *mc1r<sup>K.O.</sup>* line (where all  
421 *Mc1r* is eliminated by mutation). As discussed above both dorsal phenotypes (*asip1-*  
422 *Tg* vs *mc1r<sup>K.O.</sup>*) differed extensively thus challenging this original hypothesis. Our  
423 results suggest that melanophore lineage specification and differentiation in the dorsal  
424 skin are not fully dependent on *Mc1r* activity and thus, some other receptors,  
425 presumably other *Mcrs*, interact with *Asip1*. The presence of different *Mcrs* has been  
426 reported in several species (see introduction for references). However, we cannot  
427 exclude that some other non-melanocortin receptors could be involved in *Asip1*  
428 function, since Agouti is able to increase intracellular  $Ca^{2+}$  levels in skeletal myocytes  
429 via mechanisms that may not involve *Mcr* antagonism (Zemel et al., 1995). In mice, it

430 has been suggested that the stronger pheomelaninic phenotype of *asip* overexpressing  
431 mice carrying *mc1r* mutation might result from a  $\beta$ -arrestin-mediated mechanism  
432 leading to increased cAMP degradation, reducing the signaling to greater level than  
433 when *mc1r* is absent (Jackson et al., 2007). Such a mechanism would also be  
434 conceivable here in zebrafish.

435 Our data suggest that most precursors in the dorsal region need an *Asip1*-free  
436 environment to become melanophores but the *mc1r<sup>K.O.</sup>* phenotype suggests that only  
437 some of them seem to require a functional *Mc1r*. However, the *mc1r<sup>K.O.</sup>+asip1-Tg*  
438 phenotype is similar to the *mc1r<sup>K.O.</sup>* phenotype, suggesting that the inhibitory effects  
439 of *Asip1* on melanophores require a functional *Mc1r*.

440 We note that only the melanophores along the dorsal midline are apparently resistant  
441 to the presence of high *Asip1* levels (see schematic representation on Fig. 8).  
442 However, these melanophores are distinct in that they are localized immediately dorsal  
443 to the CNS and not in the skin; these dorsal midline cells might be insensitive to *Asip1*,  
444 for example, because they lack *mc1r* expression. Consistent with this explanation, we  
445 note that these dorsal midline melanophores are unaffected in *mc1r* mutants and the  
446 *mc1r<sup>K.O.</sup>;Asip1-Tg* combination. Furthermore, our observations indicate that these cells  
447 are likely to derive from persisting embryonic melanocytes of the early larval dorsal  
448 stripe, rather than from adult pigment stem cells. Alternatively, a trivial explanation  
449 of the difference might be that the *Asip1-Tg* shows less robust expression of *Asip1* in  
450 the adjacent tissues (CNS and/or dorsal myotome).

451 In contrast to the dorsal region, the effects of *Mc1r* dysfunction in the ventral region  
452 depend on the developmental stage. During the early post-metamorphic stages, *Mc1r*  
453 knockout induces similar effects to those observed in the dorsal region, i.e. a decrease  
454 in the density of melanophores. However, in adult animals, the effects are opposite to

those observed in the dorsal area or during the early post-metamorphic stages in the ventral skin. This we interpret as a dorsalisation of the ventral region. Therefore, functional *Mc1r* is necessary to block melanophores and xanthophores in favor of iridophores in the ventral skin of adult animals. Ventral *Asip1* levels would limit melanophore/xanthophore specification, differentiation and/or proliferation and conversely promote iridophores, but since this pathway requires the expression of *mc1r*, its absence in the mutants will allow the production of ventral melanophores and xanthophores and result in a reduction in the iridophore number. This dorsalisation phenomenon of the ventral region extends also to the ventral-most stripes, with a thickened 2V-stripe and a fully-developed 3V-stripe in the ventrum of *mc1r<sup>K.O.</sup>* mutant lines. Therefore, *Asip1*-induced inhibition of melanogenesis and melanophore differentiation *via* *Mc1r* may limit the addition of new dark stripes in the ventral region.

Finally, we also analyzed the effect of *Mc1r* dysfunction in the dorsal and ventral scales. As expected, ventral scales in WT fish lack all chromatophores but the absence of a functional *Mc1r* results in the development of ectopic melanophores and numerous xanthophores, again consistent with our interpretation of this dorsalisation of the ventral skin. However, the effect on dorsal scales was slightly different from that observed in the dorsal skin. Dorsal scales exhibit a reduction in the number of melanophore similar to that recorded in the dorsal skin but the number of xanthophores is increased dramatically. Further work will be necessary to understand the different responses to *Mc1r* absence of these progenitors in scales versus the skin.

In summary, we demonstrate that *Mc1r* is involved in the establishment of the dorso-ventral pigment pattern in zebrafish. The ventral region requires a functional *Mc1r* to block the production of melanophores and xanthophores and to promote iridophores.

480 In the dorsal region, the absence of Mc1r only results in a partial reduction in the  
481 number of melanophores and xanthophores suggesting the potential involvement of  
482 additional Mcrs in mediating the antagonistic signal of Asip1.

483

## 484 **ACKNOWLEDGEMENTS**

485 We thank Christiane Nüsslein-Volhard Lab from Max-Planck Institute (Germany) for  
486 providing the TDL358:GFP and Kita:GalTA4;UAS:mCherry transgenic lines. We  
487 would also like to thank Inés Pazos Garridos (CACTI, University of Vigo, Spain) for  
488 her assistance with confocal imaging and Pili Comesaña for her help in handling and  
489 care of the fish. This work was funded by the Spanish Economy and Competitiveness  
490 Ministry projects AGL2011-23581, AGL2014-52473R, AGL2017-89648P to JR.  
491 Partial funding was obtained from AGL2016-74857-C3-3-R to JMCR. L. Cal was  
492 supported by pre-doctoral fellowship FPI funded by Spanish Economy and  
493 Competitiveness Ministry (AGL2011-23581) and by pre-doctoral fellowship of the  
494 Spanish Personnel Research Training Program funded by Spanish Economy and  
495 Competitiveness Ministry (EEBB-C-14- 00467). P Suarez-Bregua was supported by  
496 AGL2014-52473R and AGL2017-89648P project contract. The funders had no role in  
497 study design, data collection and analysis, decision to publish or preparation of the  
498 manuscript. None of the contributing authors has any competing interests.

499

## 500 **REFERENCES**

501 Aberdam, E., Bertolotto, C., Sviderskaya, E.V., de Thillot, V., Hemesath, T.J.,  
502 Fisher, D.E., Bennett, D.C., Ortonne, J.P. and Ballotti, R. (1998) Involvement of  
503 microphthalmia in the inhibition of melanocyte lineage differentiation and of  
504 melanogenesis by agouti signal protein. *J Biol Chem* **273**, 19560–19565.

505 Agulleiro, M., Sánchez, E., Leal, E., Cortés, R., Fernández-Durán, B., Guillot, R.,  
 506 Davis, P., Dores, R.M., Gallo-Payet, N. and Cerdá-Reverte, J.M. (2013) Molecular  
 507 characterization and functional regulation of melanocortin 2 receptor (MC2R) in  
 508 the sea bass. A putative role in the adaptation to stress. *PLoS One* **8**, e65450.

509 Anelli, V., Santoriello, C., Distel, M., Köster, R.W., Ciccarelli, F.D. and Mione M.  
 510 (2009) Global repression of cancer gene expression in a zebrafish model of  
 511 melanoma is linked to epigenetic regulation. *Zebrafish* **6**, 417–424.

512 Bassett, A.R., Tibbit, C., Ponting, C.P. and Liu, J.L. (2013) Highly Efficient  
 513 Targeted Mutagenesis of Drosophila with the CRISPR/Cas9 System. *Cell Rep* **4**,  
 514 220–8.

515 Cal, L., Megías, M., Cerdá-reverter, J. , Postlethwait. J.H., Braasch, I. and Rotllant,  
 516 J. (2017) BAC Recombineering of the Agouti Loci from Spotted Gar and Zebrafish  
 517 Reveals the Evolutionary Ancestry of Dorsal–Ventral Pigment Asymmetry in Fish.  
 518 *J Exp Zool Part B Mol Dev Evol* **328**, 697–708.

519 Cal, L., Suarez-Bregua, P., Comesaña, P., Owen, J., Braasch, I., Kelsh, R., Cerdá-  
 520 Reverter, J.M., Rotllant J. (2019) Countershading in zebrafish results from an  
 521 Asip1 controlled dorsoventral gradient of pigment cell differentiation. *Sci Rep*.  
 522 **9**(1):3449. doi: 10.1038/s41598-019-40251-z.

523 Ceinos, R.M., Guillot, R., Kelsh, R.N., Cerdá-Reverter, J.M. and Rotllant, J.  
 524 (2015) Pigment patterns in adult fish result from superimposition of two largely  
 525 independent pigmentation mechanisms. *Pigment Cell Melanoma Res* **28**, 196–209.

526 Cerdá-Reverter, J.M, Agulleiro, M.J., Cortés, R., Sánchez, E., Guillot, R., Leal,  
527 E., Ferández-Durán, B., Puchol, S. and Eley, M. (2013) Involvement of  
528 melanocortin receptor accessory proteins ( MRAPs ) in the function of  
529 melanocortin receptors. *Gen Comp Endocrinol* **188**:133-6 doi:  
530 10.1016/j.ygcen.2013.01.017.

531 Cerdá-Reverter, J.M., Haitina, T., Schiöth, H.B. and Peter, R.E. (2005) Gene  
532 Structure of the Goldfish Agouti-Signaling Protein: A Putative Role in the Dorsal-  
533 Ventral Pigment Pattern of Fish. *Endocrinology* **146**, 1597–1610.

534 Cerdá-Reverter, J.M., Ling, M.K., Schiöth, H.B. and Peter, R.E. (2003) Molecular  
535 cloning, characterization and brain mapping of the melanocortin 5 receptor in the  
536 goldfish. *J Neurochem* **87**, 1354–1367.

537 Cerdá-Reverter, J.M., Ringholm, A., Schiöth, H.B. and Peter, R.E. (2003)  
538 Molecular cloning, pharmacological characterization, and brain mapping of the  
539 melanocortin 4 receptor in the goldfish: involvement in the control of food intake.  
540 *Endocrinology* **144**, 2336–2349.

541 Cortés, R., Navarro, S., Agulleiro, M.J., Guillot, R., García-Herranz, V., Sánchez,  
542 E. and Cerdá-Reverter, J.M. (2014) Evolution of the melanocortin system. *Gen*  
543 *Comp Endocrinol* **209**:3-10. doi: <http://dx.doi.org/10.1016/j.ygcen.2014.04.005>

544 Gross, J.B., Borowsky, R. and Tabin, C.J. (2009) A novel role for Mc1r in the  
545 parallel evolution of depigmentation in independent populations of the cavefish  
546 *Astyanax mexicanus*. *PLoS Genet* **5**, e1000326.



547 Guillot, R., Ceinos, R.M., Cal, R., Rotllant, J. and Cerdá-Reverter, J.M. (2012)  
548 Transient ectopic overexpression of agouti-signalling protein 1 (Asip1) induces  
549 pigment anomalies in flatfish. *PLoS One* **7**, e48526.

550 Guillot, R., Cortés, R., Navarro, S., Mischitelli, M., García-Herranz, V., Sánchez,  
551 E., Cal L., Navarro, J.C., Míguez, J.M., Afanasyev, S., Krasnov, A., Cone, R.D.,  
552 Rotllant, J. and Cerdá-Reverter, J.M. (2016) Behind melanocortin antagonist  
553 overexpression in the zebrafish brain: A behavioral and transcriptomic approach.  
554 *Horm Behav* **82**, 87–100.

555 Hirata, M., Nakamura, K., Kanemaru, T., Shibata, Y. and Kondo, S. (2003)  
556 Pigment cell organization in the hypodermis of zebrafish. *Dev Dyn* **227**, 497–503.

557 Hirata, M., Nakamura, K.I. and Kondo, S. (2005) Pigment cell distributions in  
558 different tissues of the zebrafish, with special reference to the striped pigment  
559 pattern. *Dev Dyn* **234**, 293–300.

560 Jackson, I.J., Budd, P.S., Keighren, M., McKie, L. (2007)  
561 Humanized MC1R transgenic mice reveal human specific receptor function. *Hum*  
562 *Mol Genet.* **16**(19):2341-8.

563 Kelsh, R.N. (2004) Genetics and evolution of pigment patterns in fish. *Pigment*  
564 *Cell Res* **17**, 326–336.

565 Kimmel, C.B., Ballard, W.W., Kimmel, S.R., Ullmann, B. and Schilling, T.F.  
566 (1995) Stages of embryonic development of the zebrafish. *Dev Dyn* **203**, 253–310.

567 Kobayashi, Y., Mizusawa, K., Saito, Y. and Takahashi, A. (2012) Melanocortin

568 systems on pigment dispersion in fish chromatophores. *Front Endocrinol* 3(9), 1-  
569 6.

570 Kottler, V.A., Künstner, A. and Scharl, M. (2015) Pheomelanin in fish? Pigment  
571 *Cell Melanoma Res* **28**, 355–356.

572 Le Pape, E., Passeron, T., Giubellino, A., Valencia, J.C., Wolber, R. and Hearing,  
573 V.J. (2009) Microarray analysis sheds light on the dedifferentiating role of agouti  
574 signal protein in murine melanocytes via the Mc1r. *Proc Natl Acad Sci U S A* **106**,  
575 1802–1807.

576 Levesque, M.P., Krauss, J., Koehler, C., Boden, C. and Harris, M.P. (2013) New  
577 Tools for the Identification of Developmentally Regulated Enhancer Regions in  
578 Embryonic and Adult Zebrafish. *Zebrafish* **10**, 21–29.

579 Linnen, C., Poh, Y., Peterson, B., Barret., R, Larson, J., Jensen, J. and Hoekstra,  
580 H.E. (2013) Adaptive evolution of multiple traits through multiple mutations at a  
581 single gene. *Science* **339**, 1312–1316.

582 Michaud, E.J., Bultman, S.J., Stubb,s L.J, and Woychik, R.P. (1993) The  
583 embryonic lethality of homozygous lethal yellow mice AylAy] is associated with  
584 the disruption of a novel RNA-binding protein. *Genes Dev.* **7**, 1203–1213.

585 Miller, M.W., Duhl, D.M., Vrieling, H., Cordes, S.P., Ollmann, M.M., Winkes,  
586 B.M. and Barsh, S. (1993) Cloning of the mouse agouti gene predicts a secreted  
587 protein ubiquitously expressed in mice carrying the lethal yellow mutation. *Genes*  
588 *Dev* **7**, 454–467.

589 Montague, T.G., Cruz, J.M., Gagnon, J., Church, G.M. and Valen, E. (2014)  
590 CHOPCHOP: a CRISPR/Cas9 and TALEN web tool for genome editing. *Nucleic*  
591 *Acids Res* **42**:401-7. doi: 10.1093/nar/gku410

592 Ollmann, M.M., Lamoreux, M.L., Wilson, B.D., Barsh, G.S. (1998) Interaction of  
593 Agouti protein with the melanocortin 1 receptor in vitro and in vivo. *Genes Dev* **12**  
594 (3): 316-30.

595

596 Parichy, D.M., Elizondo, M.R., Mills, M.G., Gordon, T.N. and Engeszer, R.E.  
597 (2009) Normal table of postembryonic zebrafish development: Staging by  
598 externally visible anatomy of the living fish. *Dev Dyn* **238**, 2975–3015.

599 Robbins, L.S., Nadeau, J.H., Johnson, K.R., Kelly, M.A., Roselli-Rehfuss, L.,  
600 Baack, E., Mountjoy, K.G. and Cone, R.D. (1993) Pigmentation phenotypes of  
601 variant extension locus alleles result from point mutations that alter MSH receptor  
602 function. *Cell* **72**(6):827–34.

603 Sánchez, E., Rubio, V.C. and Cerdá-Reverter, J.M. (2009) Characterization of the  
604 sea bass melanocortin 5 receptor: a putative role in hepatic lipid metabolism. *J Exp*  
605 *Biol* **212**, 3901–3910.

606 Sánchez, E., Rubio, V.C. and Cerdá-Reverter, J.M. (2010) Molecular and  
607 pharmacological characterization of the melanocortin type 1 receptor in the sea  
608 bass. *Gen Comp Endocrinol* **165**, 163–169.

609 Schiöth, H.B., Haitina, T., Ling, M.K., Ringholm, A., Fredriksson, R., Cerdá-

610 Reverter, J.M. and Klovins, J. (2005) Evolutionary conservation of the structural,  
611 pharmacological, and genomic characteristics of the melanocortin receptor  
612 subtypes. *Peptides* **26**, 1886–1900.

613 Singh, A.P., Dinwiddie, A., Mahalwar, P., Schach, U., Linker, C., Irion, U. and  
614 Nüsslein-Volhard, C. (2016) Pigment Cell Progenitors in Zebrafish Remain  
615 Multipotent through Metamorphosis. *Dev Cell* **38**, 316–330.

616 Sviderskaya, E.V., Hill, S.P., Balachandar, D., Barsh, G.S. and Bennett, D.C.  
617 (2001) Agouti signaling protein and other factors modulating differentiation and  
618 proliferation of immortal melanoblasts. *Dev Dyn* **221**, 373–379.

619 Vrieling, H., Duhl, D.M., Millar, S.E., Miller, K. and Barsh, G.S. (1994)  
620 Differences in dorsal and ventral pigmentation result from regional expression of  
621 the mouse agouti gene. *Proc Natl. Acad. Sci. U S A*. **91**, 5667–5671.

622 Wei, R., Yuan, D., Zhou, C., Wang, T., Lin, F., Chen, H., Wang, Y., Liu, J., Gao,  
623 Y. and Li, Z. (2013) Cloning, distribution and effects of fasting status of  
624 melanocortin 4 receptor (MC4R) in *Schizothorax prenanti*. *Gene* **532**, 100–107.

625 Westerfield, M. (2007) *The Zebrafish Book. A Guide for the Laboratory Use of*  
626 *Zebrafish (Danio rerio)*. 5th edn. University of Oregon Press, Eugene

627 Zemel, M.B., Kim, J., Woychik, R.P., Michaudt, E.J., Kadwell, S., Patel, I.R.  
628 and Wilkison, W.O. (1995) Agouti regulation of intracellular calcium : Role in the  
629 insulin resistance of viable yellow mice. *Proc Natl Acad Sci* **92**, 4733–4737.

630

## 631 **FIGURE LEGENDS**

### 632 **Figure 1. CRISPR/Cas9-induced mutations in the zebrafish *mc1r* gene.** (A)

633 Scheme of the *mc1r* single exon gene showing the target sites (black arrowheads: T1,  
634 T2). Coding region (CDS) are represented as white boxes and 5' UTR and 3'UTR are  
635 shown as black boxes. (B) Sequence of induced mutations in the *mc1r* gene. The first  
636 and fourth lines show the wild-type target sequences (T1 and T2). Black arrowheads  
637 label the protospacer-adjacent motif (PAM). The following lines show different  
638 induced mutations. Italic lower case letters represent inserted new sequence. The  
639 number of deleted (-) and inserted (+) bases are marked in the right side of each  
640 sequence. Selected mutations for further analysis are labeled by white arrowheads. (C)  
641 Predicted amino acid sequence encoded by generated *mc1r* variants. The first line  
642 shows the wild type protein, and following lines show the potential protein sequence  
643 of each selected mutation. Grey boxes show part conserved with the wild type (WT)  
644 sequence. Asterisk represents the stop codon. Mutation M2 generates the shortest  
645 predicted protein.

### 647 **Figure 2. The adult dorsal-ventral countershading pattern is disrupted in *mc1r*<sup>K.O</sup>**

648 Lateral (A, B), anterior-lateral (C, D), ventral-head (E, F), ventral-belly (G, H) and  
649 dorsal (I, J) views of 210 dpf WT and *mc1r*<sup>K.O</sup> zebrafish. (A, B) The pigment pattern  
650 of WT zebrafish is a striped pigment pattern with dark stripes and light interstripes.  
651 Each dark stripe has a standard nomenclature: two primary stripes are called 1D and  
652 1V, and the two secondary stripes are named 2D and 2V. The *mc1r*<sup>K.O</sup> phenotype is  
653 characterized by a darker ventrum than WT. (C, D) The striped pigment pattern looks  
654 almost unaltered in *mc1r*<sup>K.O</sup> fish. The only perceptible modification is that the *mc1r*<sup>K.O</sup>.  
655 mutant fish showed a thickened 2V-stripe and a fully-developed 3V-stripe in the

ventrum compared to WT. The darker ventrum of *mc1r<sup>K.O</sup>* than WT fish is clearly evident. (E, F) In WT, the melanophores appear in reduced numbers around the jaws and branchiostegals; however, branchiostegal, jaw and operculum regions are hyperpigmented in *mc1r<sup>K.O</sup>*. (G, H) Melanophores on the WT belly are virtually absent; thus, their ventral region shows a bright white color as a result of high numbers of iridophores in the abdominal wall. However, *mc1r<sup>K.O</sup>* shows hyperpigmentation, with increased numbers of melanophores and xanthophores in ventral skin, and the abdominal wall seems to be also affected because it appears overall more yellowish than WT. (I, J) The dorsal region is also affected in *mc1r<sup>K.O</sup>*: the WT dorsum shows more melanophores than the *mc1r<sup>K.O</sup>* dorsum. Scale bar: (A,B) 5 mm, (C,D, E, F, G, H) 1 mm and (I, J) 0.5 mm. Abbreviation: br, branchiostegal.

**Figure 3. Dorsal-ventral distribution of melanophores during metamorphosis.** (A) Distribution and density of melanophores in WT and *mc1r<sup>K.O</sup>* 15dpf fish. At this stage, *mc1r<sup>K.O</sup>* shows significantly lower density of melanophores in the dorsal region, lateral region and in the belly. (B) Distribution and density of melanophores in WT and *mc1r<sup>K.O</sup>* 30 dpf fish. At this stage, *mc1r<sup>K.O</sup>* shows significantly lower density of melanophores in the dorsal region of the head, in the dorsal region, in the lateral region, and in the belly region. Data are the mean±SEM, n=6 fish. Asterisks indicate significant differences between WT and *mc1r<sup>K.O</sup>* fish. Scale bar: (A) 200 µm, (B) 500 µm.

**Figure 4. Dorsal-ventral distribution of melanophores and xanthophores in WT and *mc1r<sup>K.O</sup>* adult fish.** (A) Lateral view of zebrafish showing the body regions selected for melanophore and xanthophore count at 210dpf. (B) Ventral view of bellies of WT and *mc1r<sup>K.O</sup>* zebrafish at 210 dpf. (C) Distribution and density of melanophores in 60 dpf WT and *mc1r<sup>K.O</sup>* fish. At this stage, *mc1r<sup>K.O</sup>* shows significantly lower density of melanophores in dorsal head, dorsal region, and black stripes 2D, 1D and 1V.

684 However, *mc1r<sup>K.O</sup>* shows significantly higher density of melanophores in the ventral  
685 region of the head. (D) Density of xanthophores in dorsal and ventral skin of WT and  
686 *mc1r<sup>K.O</sup>* 60 dpf fish. At this stage, *mc1r<sup>K.O</sup>* shows significantly higher density of  
687 xanthophores in the belly region. (E) Distribution and density of melanophores in WT  
688 and *mc1r<sup>K.O</sup>* 210 dpf fish. At this stage, *mc1r<sup>K.O</sup>* shows significantly lower density of  
689 melanophores in dorsal head, dorsal region and black stripes 2D and 1D; conversely,  
690 *mc1r<sup>K.O</sup>* shows significantly higher density of melanophores in black stripe 3V, ventral  
691 head and belly. (F) Number of xanthophores in dorsal and ventral skin of WT and  
692 *mc1r<sup>K.O</sup>* 210 dpf fish. The *mc1r<sup>K.O</sup>* fish showed highly significant lower density of  
693 xanthophores in dorsal regions and significantly higher density of xanthophores in  
694 belly region than WT. Data are the mean  $\pm$ SEM, n=7. Asterisks indicate significant  
695 differences between WT and *mc1r<sup>K.O</sup>* fish. Scale bar (A,C,E) 1mm, (B) 100  $\mu$ m.

696  
697 **Figure 5. Detection of transgenically-labelled pigment cells in WT and *mc1r<sup>K.O</sup>***  
698 **fish.** (A) Ventral view of 210 dpf WT belly. (B) Belly of 210 dpf WT fish carrying  
699 Tg(Kita:GalTA4;UAS:mCherry) transgene shows no melanophores in ventral skin.  
700 (C) Ventral view of 210 dpf *mc1r<sup>K.O</sup>* belly. (D) Belly of 210 dpf *mc1r<sup>K.O</sup>* fish carrying  
701 Tg(Kita:GalTA4;UAS:mCherry) transgene shows higher number of melanophores in  
702 ventral skin (white arrow). (E) Internal view of 210 dpf fish abdominal wall. WT  
703 ventral abdominal wall shows a white sheet of iridophores with few internal  
704 melanophores (black arrow). (F) Ventral abdominal wall of 210 dpf WT fish carrying  
705 Tg(TDL358:GFP) transgene displays a uniform sheet of iridophores. (G) Ventral  
706 abdominal wall of 210 dpf *mc1r<sup>K.O</sup>* shows a discontinuous sheet of iridophores with  
707 high number of melanophores. (H) Ventral abdominal wall of 210 dpf *mc1r<sup>K.O</sup>* fish

708 carrying Tg(TDL358:GFP) transgene exhibits a broken sheet of iridophores. Scale  
709 bars: 100  $\mu$ m.

710

711 **Figure 6. Adult *mc1r*<sup>K.O</sup> dorsal and ventral scales displayed an anomalous color**  
712 **pattern.** (A) A typical 210 dpf WT dorsal scale exhibit a pattern of melanophores  
713 (black arrowheads) and xanthophores (yellow arrowheads). (B) 210 dpf *mc1r*<sup>K.O</sup> dorsal  
714 scale exhibits a strong reduction of melanophores number (black arrowheads). (C) A  
715 typical 210 dpf WT ventral scale does not exhibit any chromatophores. (D) 210 dpf  
716 *mc1r*<sup>K.O</sup> ventral scales exhibit a pattern of melanophores (black arrowheads) and  
717 xanthophores (yellow arrowheads). Scale bars: 100  $\mu$ m.

718

719 **Figure 7. Interaction between *asip1* overexpression phenotype and *mc1r*<sup>K.O</sup> fish.**

720 Lateral (A, E, I, M), anterior-lateral (B, F, J, N), ventral-belly (C, G, K, O) and dorsal  
721 (D, H, L, P) views of 100 dpf WT, *mc1r*<sup>K.O</sup>, *asip1*-Tg zebrafish and *mc1r*<sup>K.O</sup>+*asip1*-  
722 Tg. (A) The pigment pattern of WT zebrafish shows (B) normal striped pattern, (C)  
723 light belly, and (D) dark dorsum. (E) The pigment pattern of *mc1r*<sup>K.O</sup> fish shows (F)  
724 almost normal striped pattern with a dark stripe 3V more developed and the dark stripe  
725 2D less developed than WT fish, (G) hyperpigmented belly, and (H) a lesser pigmented  
726 dorsum compared to WT. (I) The pigment pattern of *asip1*-Tg fish shows (J) almost  
727 normal striped pattern, but without dark stripe 2D, (K) light belly, and (L)  
728 hypopigmented dorsum. (M) The *mc1r*<sup>K.O</sup>+*asip1*-Tg phenotype shows the same  
729 phenotype as the *mc1r*<sup>K.O</sup> phenotype. Almost normal striped pattern with a dark stripe  
730 3V (N) more developed and the dark stripe 2D less developed than WT fish, (O)  
731 hyperpigmented belly and (P) a lesser pigmented dorsum. (Q-T) Density of  
732 melanophores in dorsal and the ventral region of WT (Q), *mc1r*<sup>K.O</sup> (R), *asip1*-Tg (S)



733 and *mc1r<sup>K.O.</sup>+asip1-Tg* (T) adult fish. Data are the mean±SEM, n=6 fish. Scale bar: (A,  
734 E, I, M) 2 mm, (B, C, D, F, G, H, J, K, L, N, O, P) 1 mm.

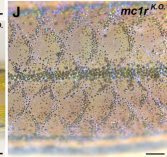
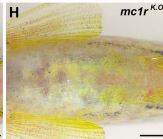
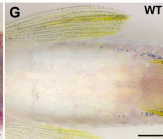
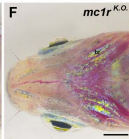
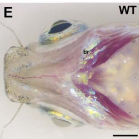
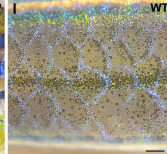
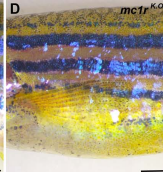
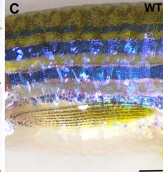
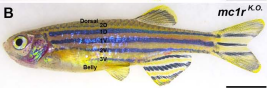
735

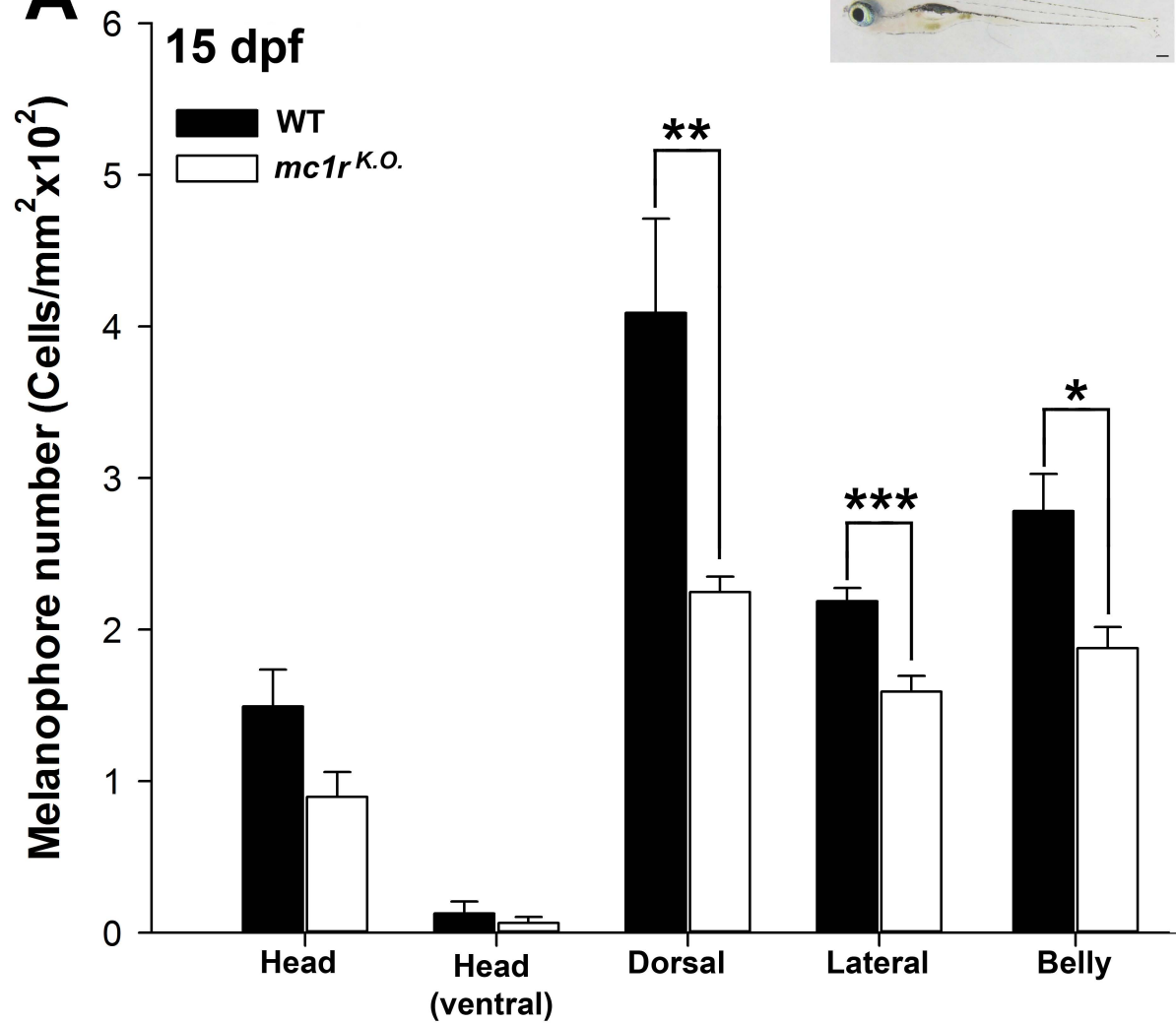
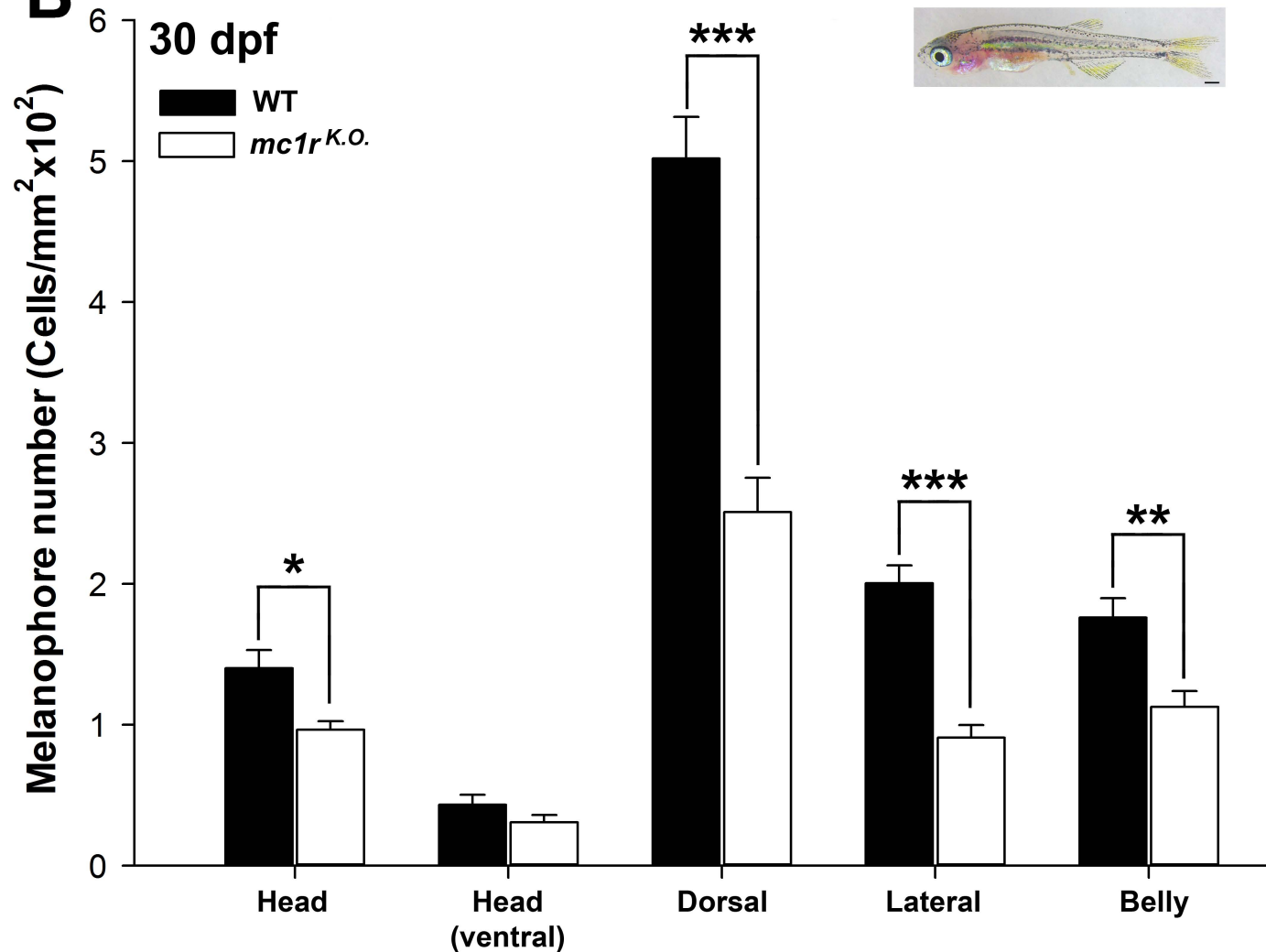
736 **Figure 8: Schematic representation of melanophore dorsal phenotypes of WT,**  
737 ***mc1r<sup>K.O.</sup>*, *asip1-Tg* and *mc1r<sup>K.O.</sup>+asip1-Tg* fish.** We propose three different  
738 melanophore cohorts in the dorsal skin of adult fish: Mc1r-free melanophores (⊗, also  
739 called Asip1-independent), melanophores expressing Mc1r (⊙, also call Mc1r-  
740 dependent), melanophores expressing Mc1r but also expressing a second Mcr (●, also  
741 called Mc1r-independent melanophores). The sum of melanophore populations  
742 expressing only Mc1r together with the melanophores that express Mc1r together with  
743 another Mcr are called Asip-1 dependent melanophores (see text for more  
744 information).

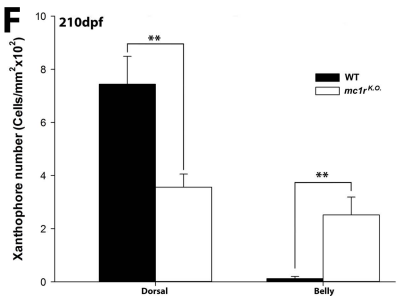
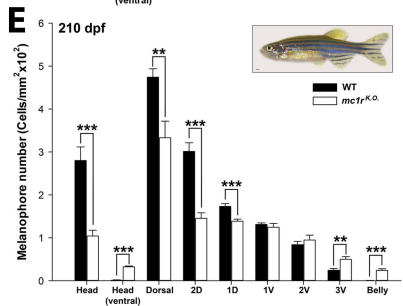
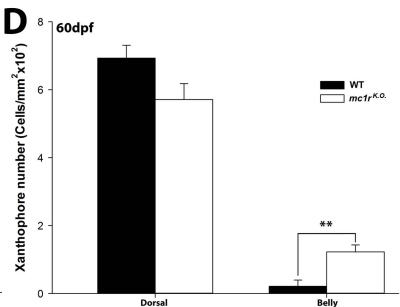
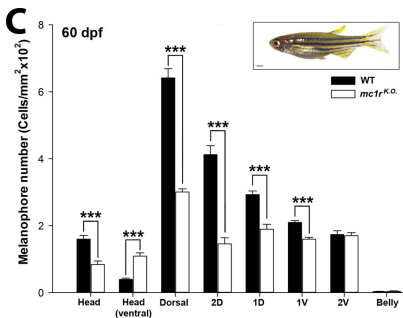
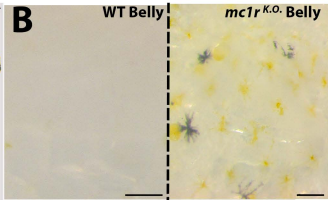
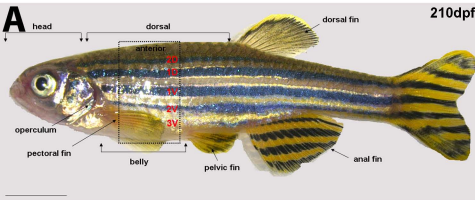
## SUPPLEMENTARY DATA

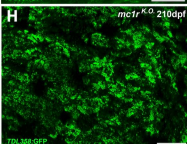
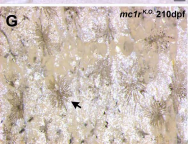
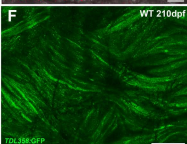
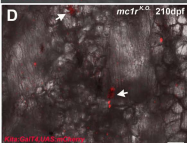
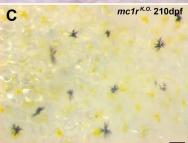
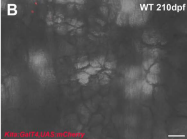
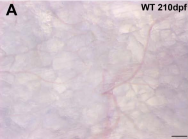
**Figure S1.** Functional Asip1/Mc1r interaction on dorsal (upper row) and ventral (lower row) scales color pattern in adult fish. (A) *mc1r<sup>K.O</sup>* dorsal scales exhibits a reduction of melanophores and xanthophore number compared to the typical adult WT fish dorsal scales. (B) *asip1-Tg* dorsal scale exhibits a substantial reduction of melanophores and xanthophore number compared to the *mc1r<sup>K.O</sup>* dorsal scales and the typical adult WT dorsal scales color pattern. (C) *mc1r<sup>K.O</sup>+asip1-Tg* dorsal scales exhibits a melanophores and xanthophore number similar to that shown by the *mc1r<sup>K.O</sup>* dorsal scales. (D) *mc1r<sup>K.O</sup>* ventral scales exhibit a pattern of melanophores and xanthophores. (E) *Asip1-Tg* ventral scale does not exhibit any chromatophores, similar to the typical ventral scale of adult WT fish. (F) *mc1r<sup>K.O</sup>+asip1-Tg* ventral scales exhibit a pattern of melanophores and xanthophores similar to that shown by the *mc1r<sup>K.O</sup>* ventral scales. Scale bars: 100  $\mu$ m.

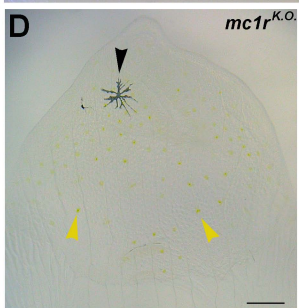
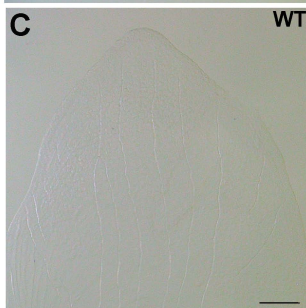
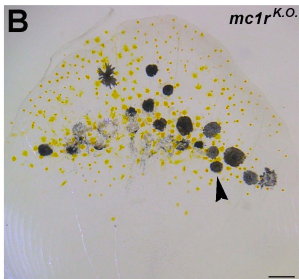
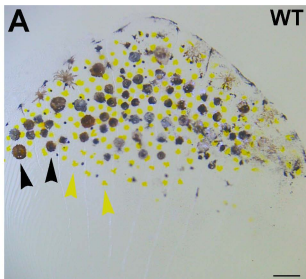




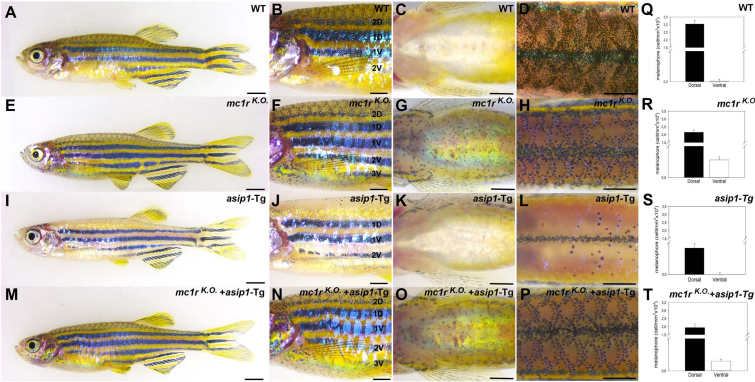
**A****B**



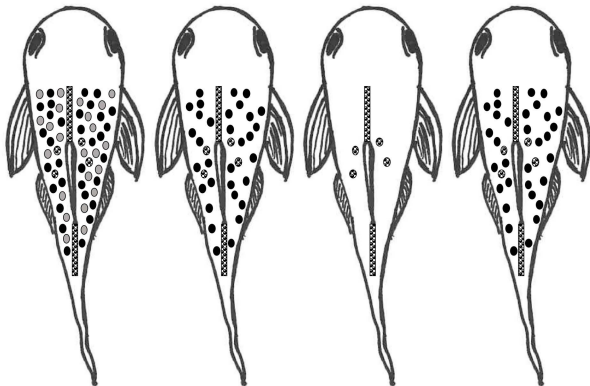








WT

*mc1r*<sup>k.o.</sup>*asip1*-Tg*mc1r*<sup>k.o.</sup> + *asip1*-Tg

- *Mc1r*-dependent melanophores
- *Mc1r*-independent melanophores
- ⊙ *Asip1*-independent melanophores
- ⊙+● *Asip1*-dependent melanophores

